

# A Novel Framework of Hybrid CNN Model with GAN Masking for Image Classification

Kadapala Anjaiah and Dr.K Sagar

Research Scholar in University College of Engineering Osmania University, Hyderabad, Telangana, India.  
Principal & Professor of Geethanjali College of Engineering and Technology, Hyderabad, Telangana, India.

**Abstract**— Processing images from satellite photography is a significant difficulty. Finding things in a satellite picture is a crucial job in this field. Since there has been a lot of study done on machine learning-based image processing, machine learning techniques may be used for this. Image processing tasks may be carried out via a multitude of machine learning-based supervised and unsupervised techniques. This research evaluated object identification systems based on machine learning using satellite photos. Finding one supervised and one unsupervised method to apply and compare across a created dataset was the aim of the study. In order to tackle these obstacles, our research used transfer learning in conjunction with multi-object identification deep learning algorithms using remotely sensed satellite data obtained on a diverse terrain. Using our recently developed dataset, five object identification techniques based on YOLO R-CNN architectures were examined via tests. A dataset of items from satellite pictures was produced specifically for the project. Both silhouette score analysis and confusion matrix analysis were used to assess the experiment's outcomes. The findings indicated that YOLOv8 had the quickest detection speed of 0.2 ms and the greatest detection accuracy of more than 90% for situations including vegetation and swimming pools. The study's findings indicate that, when it comes to object detection on satellite photos, support vector machines are more useful than k-means clustering. Hyperspectral image classification (HSIC) is challenging due to spectral similarity and variability. While 2-D CNNs use only spatial features, 3-D CNNs leverage both spatial and spectral data for better accuracy but are often computationally expensive. This study proposes an efficient 3-D CNN model using overlapping 3-D patches and a kernel function to reduce complexity. The model achieves higher accuracy and faster convergence than existing 2-D/3-D CNN methods.

**Keywords:** Satellite Images, Object Recognition, k-Means Clustering, Support Vector Machines, 3DCNN, Hyperspectral Images [HSIs], classification, kernel function

## I. INTRODUCTION

Generative Adversarial Networks (GANs) consist of two neural networks: a generator and a discriminator. GANs have the ability to reproduce samples. A Generative Adversarial Network (GAN) is used to do Semi-Supervised Learning (SSL) based on the Hilbert-Schmidt Independence Criterion (HSIC), using spectral features. In a similar manner, introduced a framework based on Generative Adversarial Networks (GAN) that combines spectral and spatial information using the Hilbert-Schmidt Independence Criterion (HSIC). Furthermore, one-dimensional customised Generative Adversarial Network (GAN) is used to create the spectral features. These features are further utilised by a Convolutional Neural Network (CNN) for feature extraction. Finally, a majority voting technique is applied using the Hilbert-Schmidt Independence Criterion (HSIC). We have recently developed that employs two generators to generate both spatial and spectral information using multiple adversarial goals.

A novel approach for HSIC involves the integration, which effectively combines high-level contextual information. This

approach was presented suggests a solution to the lack is enhanced by an auxiliary classifier, resulting in the generation of more coherent virtual training samples. issue of unbalanced data distribution across different classes, which is caused by HSIC.

### Transfer learning

The ability of a model to complete a secondary task by drawing on knowledge from a related primary job. In other words, data from one another to acquire new information that has never been labeled or observed before. Hence, transfer learning may be efficiently used in fields where depending on the availability of labelled training examples. Typically, it is believed that the source and target domains are correlated but not identical. However, it is possible for them to have distinct distributions, as is the case with HSIC.

The model learns features hierarchically in hierarchical sparse information coding (HSIC) based on deep neural networks (DNN). When trained on a variety of images, the model's bottom layers typically extract generic characteristics. As a result, a novel classifier for the intended dataset may be trained using the knowledge that these layers have acquired. As an illustration, we employed that was extensively trained using data from other HSIs. To accurately classify the target HSI, we then applied the lowest layers of this pre-trained model to the target network. The target network's upper layers are randomly initialized to gather information about its distinctive features. A small number of labelled examples from the target HSI dataset are then used to adjust the entire network. Furthermore, a workable method for pre-training and optimizing a CNN network was proposed in order to efficiently categorize new HSIs. The research combined transfer learning and data augmentation techniques in an effort to improve HSIC performance. Data in the source and target domains may vary in a number of ways, as was previously mentioned. When it comes to hyperspectral images (HSIs), for instance, two HSIs may have different sizes since they were taken using different sensors.

Heterogeneous transfer learning refers to the process of managing variances across different domains and transferring information across them.

### Active learning

Using an unlabeled sample pool, Active Learning (AL) actively increases the classifier's predicted accuracy. Active learning (AL) selects the data during each iteration, thereby improving the training dataset. Assigned to these instances by an oracle, which could be a computer or a person.

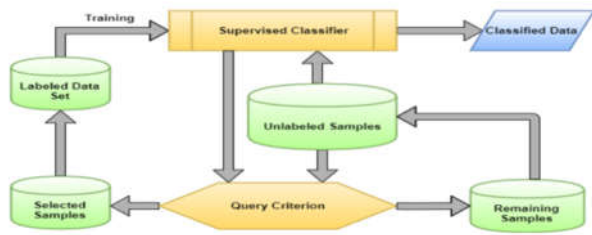


FIGURE 1: A general overview of Active Learning

Improve accuracy. Stream-based and pool-based AL frameworks can be distinguished based on how they incorporate new cases into the training set. Ranking scores that are determined by various criteria in order to evaluate the utility of the sample.

When using pool-based selection, it is crucial to provide a variety of samples in the pool to prevent duplication. When choosing or querying useful samples, the attention is often on three aspects: the heterogeneous behaviour, the performance of the model, and the representativeness of the samples. Below is a concise overview of several sampling methodologies. One possible approach to address this issue might include examining the incorporation of different learning processes outlined in section 3.10 in order to capitalise on the collective advantages. Another method involves using few-shot or K-shot learning techniques, which may make precise predictions of class labels using just a small number of labelled data. Additionally, it is necessary to prioritise the combined use of spectral-spatial characteristics of hyperspectral imagery (HSI)

Therefore, including the aforementioned factors into the creation of a new HSI framework involves effectively using the limited training samples, taking into account the combined spectral-spatial properties of HSI, and ensuring minimal computing load.

## II. RELATED WORK

The precise identification of objects in remotely sensed pictures is essential for mapping and monitoring socioeconomic and biophysical aspects [18-21]. A technique for identifying buildings from images was presented by Wang et al. [22] and included combining a CNN with an LSTM network. The pictures' features were extracted using CNN, and the spatial connections between the features were modeled by LSTM. Furthermore, a strategy based on deep learning was put out to identify ships from synthetic aperture radar (SAR) pictures [23]. The suggested technique beat various deep learning systems that were already in use, according to the findings, which were obtained by using a region proposal network (RPN) and CNN to extract features

from the photos [24-28]. In a factory, the model was used to identify objects in real time. An Auto-T-YOLO version of YOLOv4 was suggested by Sun et al. [29] to recognize objects in pictures.

Table 1: lists the constraints and performance of object identification techniques on different datasets.

Methods	Datasets	Results Obtained	Limitations
FasterR-CNN [20]	AGs-GF1 & 2	86.0%, 12 fps	Lower classification accuracy
YOLOv3 [20]	AGs-GF1 7 2	90.4%, 73 fps	Slower classification rate
YOLOv4 [19]	MS-COCO	44.5%, 64.7 fps	Requires larger computational power
YOLOv5s [21]	SIMD	5.9 ms, 61.8 mAP	Lower recognition speed as well as precision

## III. DATA SET AND FEATURES

### A. Dataset Creation:

The initial stage of the target detection process is the dataset development. Deep learning model performance and accuracy are determined by the quantity and quality of the datasets used, which makes this procedure crucial. Extensive and high-quality datasets are necessary for object recognition in photos. The development is made using large-scale datasets with deep learning algorithms that recognize objects in precise places from photos has been spurred by recent technological advancements. A vision platform called Roboflow [19-25] was used to arrange, label, and compile the photos into datasets. Ninety-two satellite photos that were marked up with the use of the multi-class categorization methodology make up the dataset. Five items may be seen in the images: a house, roads, a beach, a swimming pool, and flora. Figure 4 shows some sample photos from the collection. The dataset is divided as training, testing, validation. 61 photos along with one annotation file made up the training set; 21 photos and single annotation file made up the validation set; and 10 pictures made up the testing set. The photos underwent a few preparation operations, such as pixel data autoorientation. To improve the amount, picture augmentation was used to the training dataset. With the suggested dataset, we used a data augmentation technique to improve the models' resilience and accuracy of detection. The method uses geometric modifications and augmentations to alter the spatial orientation of pictures without altering their content. To generate a mirror image, flip the picture horizontally. To invert the image, flip it vertically.

Additionally, in order to replicate the various viewing angles of an item in the picture, the images are rotated by 90, 180, or 270 degrees. These procedures were run through 100 times in order to double the number of training photos. The most common sources of datasets in this domain are auditing events from applications or network traffic from different network devices. To assess the model, we take a look at the well-known NSL-KDD dataset: The NSL-KDD dataset, which includes both attack and benign vectors, is an improved version of the original KDD99 dataset produced by the CICS (“Canadian Institute for Cyber Security”). 42 attributes constitute the NSL-KDD dataset, and the class attribute includes five attacks that are divided into four groups: root-to-local (R2L), probing attacks, DoS (“Denial-Of-Service”), and U2R (“User-To-Root”). For multi-category attack prediction, 5 classes including the Normal category have been employed in this dataset.

#### IV. METHODOLOGY

##### A. Proposed Methodology:

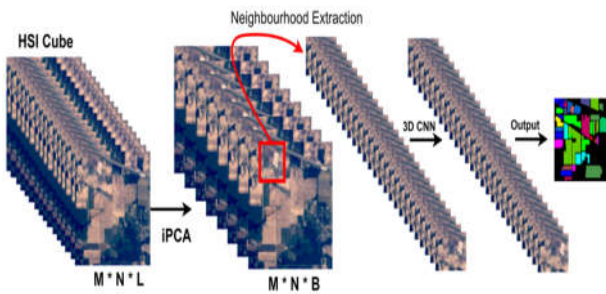


Fig 2. Process flow diagram.

Assuming a Hyperspectral Image HSI pixels demonstrate significant similarities across different classes, substantial variety within the same class. Additionally, there are instances when areas overlap and are nested inside each other. In order to address the aforementioned problems, the technique of independent principal component analysis (iPCA). To transfer the HSI cube to the model, it is necessary to partition it into tiny 3D spatial patches that overlap. The ground labels are then generated based on the centre pixel of each patch, as seen in Figure 1. Subsequently, these acquired characteristics are subjected to an activation function, which creates nonlinearity. Table 2 : 3D CNN

Layer	Output Shape	Parameters
Input Layer	(11,11,20,1)	0
Conv3D-1 (Conv3D)	(9,9,14,8)	512
Conv3D-2 (Conv3D)	(7,7,10,8)	5778
Conv3D-3 (Conv3D)	(5,5,8,32)	12365
Conv3D_4 (Conv3D)	(3,3,6,64)	52369
Flatten_1 (Flatten)	(3456)	0
Dense_1 (Dense)	(256)	884992
Dropout_1 (Dropout)	(256)	0
Dense_2 (Dense)	128	32897
Dropout_2 (Dropout)	128	0
Dense_3 (Dense)	Classes	774

Four 3D convolutional layers are used before the flatten layer to enhance the amount of spatial-spectral feature maps.

This ensures that the model can effectively differentiate spatial information across various spectral bands without any loss. Additional information on the suggested model may be seen in Table 2. The 3D CNN model we propose has a total of 994,166 tune-able weights, which serve as parameters. This specifically examines a single-stream approach that is comparable to the existing research. Regardless of whether classification tasks and exhibits rapid convergence. However, it may also result in overfitting to some degree. Various regularisation strategies, including dropout, overfitting problems. Additionally, various alternative targets have shown superior performance compared to the usual cross-entropy. Utilising image processing methods, the quality of information may be enhanced by analysing satellite pictures at varying spectral and spatial resolutions. Classification is a crucial undertaking in remote sensing applications. Performing image classification on fused pictures yields superior outcomes compared to the original data. Utilising numerous source image data for processing enhances the categorisation accuracy of remote sensing pictures. The fusion-based classification process consists of five stages: image enhancement, fusion, segmentation, feature extraction, and classification. Image enhancement is performed as a preprocessing step to fix intensity, improve edges, and remove noise. Image fusion is performed to combine two pictures with varying resolutions into a single image, with the aim of enhancing accuracy. Subsequently, the resulting fused picture is segmented using an unsupervised clustering technique. Next, distinct characteristics are retrieved and used to train the classifier. Ultimately, the picture is categorised to get diverse land cover data. The evaluation of this classification system is conducted using fused pictures from the Landsat collection.

An HSI is represented as  $X \in \mathbb{R}^{L \times (N \times M)}$ , where each of the  $N \times M$  pixels has  $L$  spectral bands and a class label. To reduce redundancy, iPCA compresses bands from  $L$  to  $B \ll L$  without altering spatial dimensions. The HSI is divided into overlapping 3D patches  $P \in \mathbb{R}^{S \times S \times B}$ , centered on each pixel. Each patch is labeled by its center. The total number of patches is  $(M-S+1) \times (N-S+1) \times (L-S+1)$ .

$$v_{i,j}^{x,y,z} = \mathcal{F} \left( \sum_{\tau=1}^{\delta} \sum_{\lambda=-\nu}^{\nu} \sum_{\rho=-\gamma}^{\gamma} \sum_{\phi=-\delta}^{\delta} w_{i,j,\tau}^{\lambda,\rho,\phi} \times v_{(i-1),\tau}^{(x+\lambda),(y+\rho),(z+\phi)} + b_{i,j} \right)$$

Patches are passed through a 3D convolution layer, followed by activation to extract nonlinear features. The output at position  $(x,y,z)$  in layer  $iii$ , feature map  $jjj$ , is  $v_{i,j}^{x,y,z}$ .

#### V. EXPERIMENTS AND MODEL EVALUATION

This section provides an overview of several benchmark actual hyperspectral imaging (HSI) datasets that were used in this research. Various airborne and satellite sensors are being used to collect these datasets.

Additionally, there are the Pavia University and Pavia Centre datasets collected using the ROSIS sensor, the Botswana dataset acquired using the Satellite Hyperion sensor. The evaluation of information from ROSIS and Hyperion sensors poses a more difficult classification challenge compared to AVIRIS sensor datasets. This is primarily due to the presence of complex urban classifications and nested areas.

TABLE 3: Summary of the HSI datasets.

Dataset	Dimension	Classes	Wave-length
Botswana	512 X 217	13	400-2500
Landsat	1496 × 256	16	400-2500
Bhuvan	610 X 610	12	360-2600
Google Earth	1096 X 1096	9	430-860
QuickBird	145 X 145	9	430-860
Indian Pines	610 X 610	8	400-1260

The Training samples, which make up 70% of the total population, are then separated into a 50/50% ratio for the Training and Validation sets.

Verifying the Precision of Class Categories

- 1: The Check Accuracy algorithm
- 2: Set up a counter variable to keep track of the number of correctly and incorrectly classified images.
- 3: Retrieve the first assigned classifications for the picture
- 4: Retrieve the anticipated label outcomes for the same picture acquired from the classifiers.
- Iterate 5 times,
- 5: starting from 1 and ending at the maximum number of blocks for the picture.
- 6: For every class category.
- 7: if the original label and anticipated label are the same
- 8: Increase the counter for accurately classifying the related class.
- 9: otherwise
- 10: Increase the number for incorrectly classifying the appropriate class
- 11: Terminate the if statement. 12: Terminate the for loop.
- 13: Compute the % accuracy for each class category individually.

Compute the mean accuracy across all class categories.

The event concludes at 15:00. Based on these numbers, it can be inferred that the suggested model reached convergence at around 20 epochs.

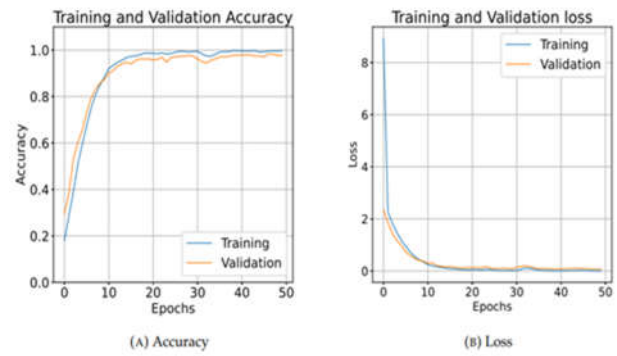


FIGURE 3: The accuracy and loss values over 50 epochs.

The experimental findings presented in this study were acquired using Google Colab, an online platform that allows for the execution of Python environments with high-speed internet connectivity. Google Colab offers the ability to run several versions of Python, access to a Graphical Processing Unit (GPU).

All models, including hybrid models, have a learning rate of 0.001 to guarantee a fair comparison. With the exception of the output layer, which uses Softmax as its activation function, all other layers use Relu. In order to minimize computational load, the 15 most informative bands for each experiment were chosen using PCA, with the patch size set to 15. A 5-fold cross-validation procedure is used to select the training, validation, and test sets for all experimental results. Specifically, 25%, 25%, and 50% of the samples are assigned between the various classes in the samples if the patch size is too small. Because of this, the final result in both cases will have a higher percentage of misclassification, which will lead to subpar generalization performance. As a result, before the final experimental setup, a suitable patch size must be determined. A set of criteria is used to determine the patch size that is used in these studies.

$$\text{Precision} = \text{TP} / (\text{TP} + \text{FP})$$

$$\text{Recall} = \text{TP} / (\text{TP} + \text{FN})$$

$$\text{Accuracy} = (\text{TP} + \text{TN}) / (\text{TP} + \text{FP} + \text{TN} + \text{FN})$$

$$\text{F-measure} = 2 \times \text{Precision} \times \text{Recall} / (\text{Precision} + \text{Recall})$$

## VI. RESULTS AND DISCUSSION

Dataset	Technique	Accuracy	Proposed Technique	Accuracy
Landsat	CNN	93.00 %	HCNN	96.23 %
RGB Satellite	CNN	92.43 %	HCNN	95.23 %
HSS Sensor	CNN	92.85 %	HCNN	96.28 %
Bhuvan	CNN	94.23 %	HCNN	96.58 %

TABLE 4 COMPARISON OF RESULTS

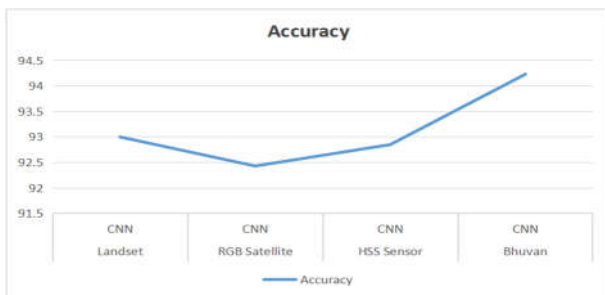
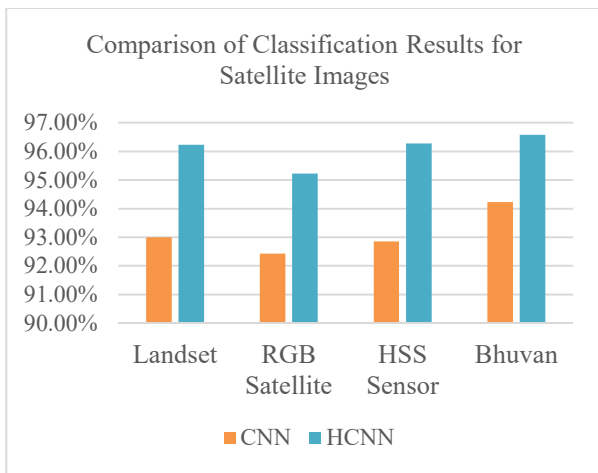


Fig .4.: Accuracy for Multiple data set using CNN

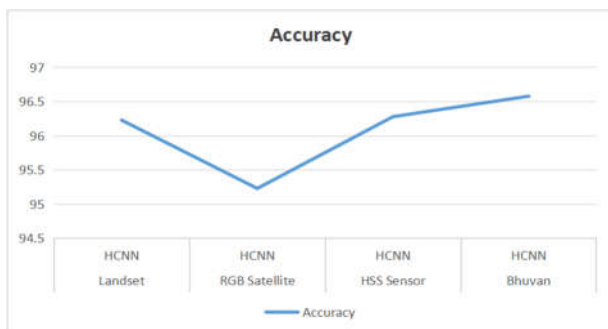


Fig .5.: Accuracy for Multiple data set using HCNN

The Gesture Recognition Project has successfully developed a functional and interactive system that can instantly recognize and interpret hand gestures. The system uses computer vision and deep learning models to accurately identify and classify various gestures, providing users with an alternative to manual interaction. The integration of the PyQt5 graphical user interface (GUI) provides interaction and rapid feedback, improving the overall user experience. The system’s ability to translate gestures such as “hello,” “thank you,” and “I love you” is an important step towards creating easy-to-use communication tools, especially for people with hearing or speech impairments. Although this system has great promise, issues such as lighting, background noise, and hand placement still affect the accuracy and reliability of directional information. This technology has established a solid foundation for cognitive navigation, which has been used in a variety of applications, including healthcare, gaming, education, and augmented reality. The system now allows for seamless integration into a conference environment, making it ideal for future assistive technology,

security, and IoT devices. The ability to use gestures to control devices without physical contact makes the body particularly useful in medical facilities where inputs like keyboards or screens are normally used, or for people with disabilities where grey touch is not a good fit. There are many areas where the project can be improved and expanded going forward. Firstly, the gesture recognition model can be expanded to recognize more descriptive and detailed information, allowing the system to meet communication needs. This could include multi-hand detection, which can recognize gestures involving both hands simultaneously. Furthermore, solving environmental issues such as lighting changes and complex backgrounds will increase the accuracy and reliability of the system. Exploring the use of depth sensors or infrared cameras could help solve these problems and provide consistent performance across different situations. or wearable devices. This would increase the mobility of the technology, making the job of the viewer easier. Integration with IoT devices and smart home devices could also be interesting, such as using gestures to control lights, appliances or security. You could also look into gesture-based security, which would provide a new and secure way to authenticate users. This could be done by optimizing the underlying machine learning model or using faster hardware such as GPUs or edge computing to make instructions more efficient. The system could also benefit from expanding its gestures to support more languages and gestures, such as different languages, making the device more usable and accessible to an international audience. Integrating technology with interactions such as voice or eye tracking will lead to the development of multimodal systems that provide more information and adapt to the user. By combining gestures with voice commands or visual cues, the system could provide greater understanding and flexibility, especially in environments where protection or non-invasive control is not important. The project has made significant progress in gesture recognition, with many opportunities for improvement and expansion. This system has the potential to change the way we interact with technology, making it easier, more accessible, and adaptable to the needs of different users in many ways by addressing current limitations and exploring new applications.

## VII. CONCLUSION

The study demonstrates that classification accuracy in satellite image analysis can be significantly improved through a block-based approach and effective feature extraction techniques. The integration of PCA and GLCM enables the capture of both color and texture information, essential for handling the complexity of high-resolution images. Additionally, careful selection of block size and feature quantity plays a critical role in optimizing performance. Overall, the results validate that combining spatial segmentation with holistic feature extraction enhances the efficiency and accuracy of remote sensing classification tasks. Classification performance is evaluated using various classifiers on 8×8 pixel blocks, with accuracy influenced by feature type, number, computation time, and classifier settings. PCA (color) and GLCM (texture) improve results, especially when combined. Block-based methods enhance accuracy in satellite image classification, with block size and feature count playing key roles.

## VIII. REFERENCES

- [1] K. Vani, "Satellite Image Processing," IEEE, Fourth International Conference on Signal Processing, Communication and Networking (ICSCN), vol. 1, no. 4, p. 53, 2017.
- [2] Kadapala Anjaiah and K. Sagar, "Transfer learning in conjunction with multi-object detection using YOLO RCNN," *The International Journal of Interdisciplinary Organizational Studies*, vol. 19, no. 1, pp. 897–907, Jan.–Jun. 2024.
- [3] Muhammad Ahmad, Adil Mehmood Khan, Manuel Mazzara, Salvatore Distefano, Mohsin Ali, and Muhammad Shahzad Sarfraz, "A Fast and Compact 3-D CNN for Hyperspectral Image Classification," *IEEE Geoscience and Remote Sensing Letters*, vol. 19, DOI: 10.1109/LGRS.2020.3043710, 2020
- [4] Kadapala Anjaiah and K. Sagar, "Using Generative Adversarial Networks (GAN) to correct banding errors in satellite images," *International Journal of Techno-Engineering (IJTE)*, vol. XVI, no. II, pp. 242–253, May 2024. [Online]. Available: <http://ijte.uk/>
- [5] M. Kumar, "Digital image processing," *Satellite Remote Sensing and GIS Applications in Agricultural Meteorology*, pp. 81–102, 2004.
- [6] M. Kumar, "Digital Image Processing of Remotely Sensed Satellite Images for Information Extraction," *Proceedings of the Conference on Advances in Communication and Control Systems-2013*, pp. 406–410, 2013.
- [7] N. Kumar, "Digital Image Processing for Image Enhancement and Information Extraction," *Society of Photo-Optical Engineers*, vol. 199, pp. 9–19, 1980.
- [8] R. Aedla, "Satellite Image Contrast Enhancement Algorithm based on Plateau Histogram Equalization," *IEEE Region 10 Symposium*, pp. 213–218, 2014.
- [9] S. S. Al-amri, N. V Kalyankar, and S. D. Khamitkar, "Contrast Stretching Enhancement in Remote Sensing Image," *BIOINFO Sensor Networks*, vol. 1, no. 1, pp. 6–9, 2011.
- [10] P. Bidwai and D. J. Tuptewar, "Resolution and contrast enhancement techniques for grey level, color image and satellite image," *Proceedings - IEEE International Conference on Information Processing, ICIP 2015*, pp. 511–515, 2016.
- [11] P. Kaushik and Y. Sharma, "Comparison of different image enhancement techniques based upon Psnr & Mse," *International Journal of Applied Engineering Research*, vol. 7, no. 11, pp. 2010–2014, 2012.
- [12] T. Blaschke, "Object based image analysis for remote sensing," *ISPRS Journal of Photogrammetry Remote Sensing*, vol. 65, no. 1, pp. 2–16, 2010.
- [13] W. Xiaoyun, Y. Weiqi, and C. V. Group, "Human Ear Recognition Based on Block Segmentation," *IEEE*, pp. 262–266, 2009.
- [14] X. Sun, L. Zhang, H. Yang, T. Wu, Y. Cen, and Y. Guo, "Enhancement of Spectral Resolution for Remotely Sensed Multispectral Image," *IEEE Journal of Selected Topics in Applied Earth Observations and Remote Sensing*, vol. 8, no. 5, p.
- [15] I. Lee and T. Choi, "Accurate Registration using Adaptive Block Processing for Multi-spectral Images," *IEEE Transactions On Circuits And Systems For Video Technology*, no. c, pp. 1–11, 2013.
- [16] A. A. G. Veenadevi.S.V., "Fixed Range Block Segmentation and Classification for Fractal Image Compression of Satellite Imageries," *IEEE Fifth International Symposium on Electronic System Design*, no. 1, pp. 1–4, 2014.
- [17] R. R. S OudayaCoumar, R.Aravindraja, S.Arulambalam, Naaraayan and R. S. P.Prasad, "Contrast Enhancement Of Satellite Images Using Advanced Block Based DWT Technique," *IEEE International Conference On Recent Trends In Information Technology*, 2016.
- [18] L. I. Smith, "A tutorial on Principal Components Analysis," *Computer Science Technical Report No. OUCS-2002-12*, 2002.
- [19] T. Celik, "Unsupervised Change Detection in Satellite Images Using Principal Component Analysis and k-Means Clustering," *IEEE Geoscience And Remote Sensing Letters*, vol. 6, no. 4, pp. 772–776, 2009.
- [20] C. Muniyati, "Use of Principal Component Analysis ( PCA ) of Remote Sensing Images in Wetland Change Detection on the Kafue Flats , Zambia," *Geocarto International*, vol. 19, no. 3, pp. 11–22, 2008.
- [21] T. Blaschke, "Object based image analysis for remote sensing," *ISPRS Journal of Photogrammetry and Remote Sensing*, vol. 65, no. 1, pp. 2–16, 2010.
- [22] S. V. S. Prasad and I. V. M. Krishna, "Classification of Multispectral Satellite Images using Clustering with SVM Classifier," *International Journal of Computer Applications*, vol. 35, no. 5, pp. 32–44, 2011.